

Previously unknown class of metalorganic compounds revealed in meteorites

Alexander Ruf^{a,b,1}, Basem Kanawati^a, Norbert Hertkorn^a, Qing-Zhu Yin^c, Franco Moritz^a, Mourad Harir^{a,b}, Marianna Lucio^a, Bernhard Michalke^a, Joshua Wimpenny^c, Svetlana Shilobreeva^d, Basil Bronsky^d, Vladimir Saraykin^{d,e}, Zelimir Gabelica^f, Régis D. Gougeon^g, Eric Quirico^h, Stefan Ralewⁱ, Tomasz Jakubowski^j, Henning Haack^{k,l}, Michael Gonsior^m, Peter Jenniskens^{n,o}, Nancy W. Hinman^p, and Philippe Schmitt-Kopplin^{a,b,1,2}

^aResearch Unit Analytical BioGeoChemistry, Helmholtz Zentrum München, 85764 Neuherberg, Germany; ^bAnalytical Food Chemistry, Technische Universität München, 85354 Freising-Weihenstephan, Germany; ^cDepartment of Earth and Planetary Sciences, University of California, Davis, CA 95616; ^dVernadsky Institute of Geochemistry and Analytical Chemistry, Russian Academy of Sciences, 119991 Moscow, Russia; ^eResearch Institute of Physical Problems named after F. V. Lukin, 124460 Moscow, Russia; ^fUniversité de Haute Alsace, École Nationale Supérieure de Chimie de Mulhouse, F-68094 Mulhouse Cedex, France; ^gUMR Procédés Alimentaires et Microbiologiques, Université de Bourgogne/AgroSupDijon, Institut Universitaire de la Vigne et du Vin Jules Guyot, 21000 Dijon, France; ^hUniversité Grenoble Alpes/CNRS-Institut National des Sciences de l'Univers, Institut de Planétologie de Grenoble, UMR 5274, Grenoble F-38041, France; ⁱSR-Meteorites, 12681 Berlin, Germany; ^jDrohobycka 32/6, Wrocław 54-620, Poland; ^kSection for Geobiology and Minerals, Natural History Museum of Denmark, University of Copenhagen, DK-1350 Copenhagen K, Denmark; ^lMaine Mineral and Gem Museum, Bethel, ME 04217; ^mChesapeake Biological Laboratory, University of Maryland Center for Environmental Science, Solomons, MD 20688; ⁿSETI Institute, Mountain View, CA 94043; ^oNASA Ames Research Center, Moffett Field, Mountain View, CA 94035; and ^pUniversity of Montana, Missoula, MT 59812

Edited by Jerrold Meinwald, Cornell University, Ithaca, NY, and approved January 26, 2017 (received for review October 6, 2016)

The rich diversity and complexity of organic matter found in meteorites is rapidly expanding our knowledge and understanding of extreme environments from which the early solar system emerged and evolved. Here, we report the discovery of a hitherto unknown chemical class, dihydroxymagnesium carboxylates $[(OH)_2MgO_2CR]^-$, in meteoritic soluble organic matter. High collision energies, which are required for fragmentation, suggest substantial thermal stability of these Mg-metalorganics (CHOMg compounds). This was corroborated by their higher abundance in thermally processed meteorites. CHOMg compounds were found to be present in a set of 61 meteorites of diverse petrological classes. The appearance of this CHOMg chemical class extends the previously investigated, diverse set of CHNOS molecules. A connection between the evolution of organic compounds and minerals is made, as Mg released from minerals gets trapped into organic compounds. These CHOMg metalorganic compounds and their relation to thermal processing in meteorites might shed new light on our understanding of carbon speciation at a molecular level in meteorite parent bodies.

metalorganic chemistry | meteorites | astrochemistry | Fourier transform ion cyclotron resonance mass spectrometry | organic evolution

The molecular diversity of extraterrestrial organic matter in carbonaceous chondrites has been studied by means of both targeted (1–4) and nontargeted (5–7) analytical methodologies, which are complementary to each other. The targeted approach focuses on molecules of biological/prebiotic interest in greater detail, such as amino acids, nucleobases, or carbohydrates (8), overlooking other analytes. In the nontargeted approach all analytes are globally profiled to gain comprehensive information. As such, holistic nontargeted analyses of meteoritic soluble organic matter revealed a much higher degree of molecular diversity than that found in any organic matter of terrestrial origin, as observed in Murchison (5, 6). The Murchison meteorite (CM2 type, where CM refers to Mighei-type carbonaceous chondrite) is the most investigated meteorite, typically seen as an example of abiotic organic complexity and a model of the processes that occurred inside its asteroid parent body (5).

Few metalorganic compounds have hitherto been described in the meteoritic context (9), despite the close proximity and intercalation of the mineral and organic phases in meteoritic materials. Fioroni predicted the identification of metalorganic species in measureable quantities; however, these have not been detected yet, either by spectroscopic techniques or upon meteorite analyses. Carbonaceous meteorites, such as Murchison (CM2) or Orgueil (CI1), are heterogeneous in organic molecular species

and their abundances (10, 11). These organic materials, including carboxylic compounds, are known to be mixed with Mg-rich phyllosilicates (11). The interaction of organic matter and minerals, especially clay minerals, plays an important role in the evolution of meteoritic organic matter via catalytic effects (12).

Mg is one of the most abundant elements in the solar system (13) and is an important component in many common rock-forming minerals. Furthermore, relative to other elements in the first three groups of the periodic table, Mg offers the highest propensities of forming metalorganic compounds (14), for example chlorophyll or Grignard reagents. Classical metalorganic compounds with a covalent Mg–C bond exhibited high binding energies with a distinct thermal robustness and an appreciable photostability (15). Mg commonly occurs as a divalent cation that is coordinated to six water molecules or other oxygen-containing

Significance

In this study we report the discovery of a previously unrecognized chemical class, dihydroxymagnesium carboxylates, $[(HO)_2MgO_2CR]^-$, gained from nonterrestrial meteoritic analyses. The existence of such low-coordination organomagnesium anionic compounds expands our knowledge and understanding of extreme environments from which the early solar system emerged and has evolved. The appearance this CHOMg chemical class extends the previously investigated vast diversity of CHNOS groups in meteoritic soluble organics. Experimental evidence is given for the connection between the evolution of organic compounds and minerals. These thermostable compounds might have contributed to the stabilization of organic molecules on a geological time scale, which emphasizes their potential astrobiological relevance.

Author contributions: A.R. and P.S.-K. designed research; A.R., B.K., N.H., M.H., Z.G., R.D.G., S.R., H.H., M.G., P.J., N.W.H., and P.S.-K. performed research; A.R., B.K., Q.-Z.Y., M.H., B.M., J.W., S.S., B.B., V.S., E.Q., T.J., and P.S.-K. contributed new reagents/analytic tools; A.R., B.K., Q.-Z.Y., F.M., M.L., B.M., J.W., S.S., B.B., V.S., E.Q., T.J., and P.S.-K. analyzed data; and A.R., B.K., N.H., Q.-Z.Y., F.M., M.H., M.L., B.M., J.W., S.S., B.B., V.S., Z.G., R.D.G., E.Q., S.R., T.J., H.H., M.G., P.J., N.W.H., and P.S.-K. wrote the paper.

The authors declare no conflict of interest.

This article is a PNAS Direct Submission.

Freely available online through the PNAS open access option.

¹A.R. and P.S.-K. contributed equally to this work.

²To whom correspondence should be addressed. Email: schmitt-kopplin@helmholtz-muenchen.de.

This article contains supporting information online at www.pnas.org/lookup/suppl/doi:10.1073/pnas.1616019114/-DCSupplemental.

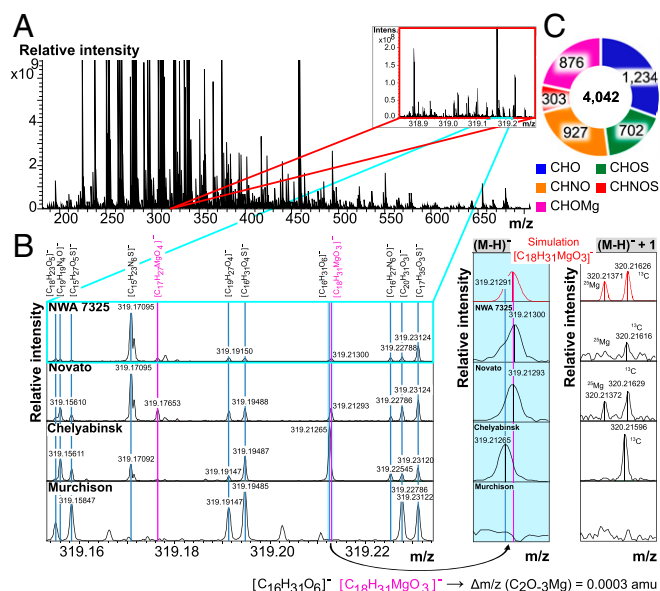


Fig. 1. Detection of the CHOMg chemical space. Negative ionization mode ESI-FT-ICR mass spectrum of an ungrouped achondrite (NWA 7325) is shown (A). It is aligned together with two ordinary chondrites (Novato and Chelyabinsk) and a carbonaceous chondrite meteorite (Murchison) by CHNOS compounds (B). Some distinct mass peaks were detected that are nonaligned and represent CHOMg compounds (pink labels). Less than one electron mass difference ($\Delta m/z = 0.0003$ amu) between the isobaric molecule ions $[\text{C}_{16}\text{H}_{31}\text{O}_6]^-$ and $[\text{C}_{18}\text{H}_{31}\text{MgO}_3]^-$, with the corresponding mass difference of $\text{C}_2\text{O}_3\text{Mg}$, requires an ultrahigh mass resolving power and high mass accuracy to enable unambiguous differentiation between the CHNOS and the CHOMg chemical spaces. The second most abundant CHOMg isotopologue, here at $m/z = 320$, consists of two peaks (^{25}Mg and ^{13}C) of comparable amplitude. The specific presence of $[\text{C}_{18}\text{H}_{31}\text{MgO}_3]^-$ is confirmed in NWA 7325 and Novato but excluded in Chelyabinsk and Murchison meteorites, which only display the single ^{13}C -based peak and no second isotopologue mass peak at $m/z = 320$. (C) Relative abundances of NWA 7325 chemical species are depicted.

ligands (16). Meteorites contain Mg-rich minerals (Fig. S1) (17) and complex organic compounds (1, 5), which are thought to evolve chemically, not simultaneously, in the early solar system (18, 19). For example, Fischer-Tropsch-type (FTT) reactions are believed to play an important role in providing pathways to form (complex) organic molecules. The reacting molecules in FTT reactions are CO , H_2 , and inorganic minerals as catalysts (20). Another hypothesis for organic matter formation is the mineral alteration by aqueous alteration (18). In both cases, minerals, including those that bear Mg (21), have a potential consequence on the organic chemistry in space.

Here, we demonstrate the occurrence and remarkable diversity of previously unrecognized CHOMg compounds within meteoritic soluble organic matter and present the chemical class of dihydroxymagnesium carboxylates, followed by a discussion of their chemical properties and reactivity. The exceptional molecular diversity makes meteorites ideal samples to elucidate fundamental chemical reactivity of organic compounds. Additionally, CHOMg signatures can be related to meteoritic thermal history and fractionation processes.

Results and Discussion

Evaluating the CHOMg Chemical Space. Our methods and processes for conducting electrospray ionization Fourier transform ion cyclotron resonance mass spectrometry (ESI-FT-ICR-MS) on soluble organics in meteorites are described in *Materials and Methods* and in *SI Materials and Methods*. To understand the

nature of previously unassigned peaks, we studied 61 meteorites with different petrologic types, covering a wide range of meteorite classes (Table S1). The selected representative meteorites include achondrite Northwest Africa 7325 [NWA 7325, ungrouped (22)], ordinary chondrites Novato and Chelyabinsk (23, 24), and carbonaceous chondrite Murchison [CM2 (5)].

The mass spectra of the ungrouped achondrite NWA 7325 show a very dense CHNOS space of soluble organic compounds, comparable to ordinary chondrites (Fig. 1). Recurrent patterns of 876 unassigned mass peaks were discovered to which we assigned CHOMg formulas (Fig. 1). These mass peaks accounted for 22% of peaks in the soluble organic matter of NWA 7325, 26% in Novato, and 24% in Chelyabinsk, all of which underwent significant heating during petrogenesis, but only 2% in the comparatively primitive meteorite Murchison; absolute quantities are not directly accessible via ESI. Nevertheless, CHO and CHOMg compounds are observed in almost equal mass peak counts n for thermally stressed meteorites [$n(\text{CHO}):n(\text{CHOMg}) \approx 1:1$]. CHO compounds represent the major soluble organic compounds in ordinary chondrites, ranging up to ~ 300 ppm (1). Thus, CHOMg compounds are expected to be in a similar concentration range.

The unambiguous distinction between the CHNOS and the CHOMg chemical spaces requires an extremely high mass resolving power ($R > 10^6$) and mass accuracy (< 200 ppb, Fig. 1) to differentiate mass differences less than the mass of an electron. At lower mass resolving power, CHOMg compositions would be largely occluded by merging with the CHNOS compositional space. To avoid any alignment error due to this m/z overlap, CHNOS compounds are shown to reveal the precise internal calibration (Fig. 1). The $^{24/25/26}\text{Mg}$ isotopic fine structure analysis validated the existence of C-, H-, O-, Mg-based compositions (Fig. 1 and Fig. S2).

The diversity of CHOMg species within soluble organic matter of NWA 7325 highlights the complex chemical space that is occupied by these metalorganic compounds (Fig. 2 and Fig. S3). This van Krevelen-type representation shows several extended, methylene-based fairly complete homologous series (Fig. S3). The absence of odd-even preferences in alkyl chains testifies to a nonbiological origin of CHOMg compounds (25). Biological synthesis of fatty acids or general aliphatic chain molecules is usually a C_2 unit propagation process (26). Therefore, the extraterrestrial origin (C_1 step chemosynthesis) can be distinguished from a terrestrial synthesis environment. Compounds bearing four oxygen atoms (MgO_4R^- , with $\text{R} = \text{hydrocarbon } \text{C}_x\text{H}_y$, and $x, y \in \mathbb{N}$)

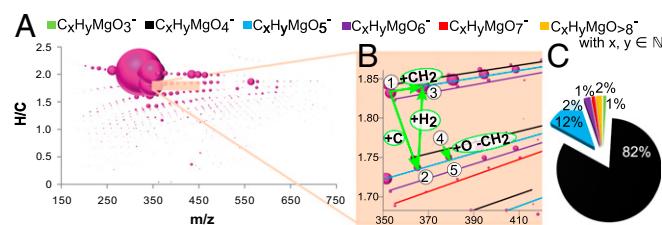


Fig. 2. Characteristics of the CHOMg chemical space. CHOMg chemical compositions of NWA 7325 soluble organic matter are depicted by mass-edited H/C ratio, for the complete (A) and zoomed-in compositional space (B), illustrating the density of fairly complete homologous series within the CHOMg compositional space. The bubble size represents the relative intensity of the mass peaks. The detailed arrangement of CHOMg compounds allows visualization of nominal elemental/molecular transformations, with examples provided (circled numbers: ①, $\text{C}_{18}\text{H}_{33}\text{MgO}_5^-$; ②, $\text{C}_{19}\text{H}_{33}\text{MgO}_5^-$; ③, $\text{C}_{19}\text{H}_{35}\text{MgO}_5^-$; ④, $\text{C}_{21}\text{H}_{37}\text{MgO}_4^-$; and ⑤, $\text{C}_{20}\text{H}_{35}\text{MgO}_5^-$). (C) Relative abundances of these Mg-metalorganics, shown in different colors (B and C), demonstrate the dominance of the MgO_4R^- molecular subspace, with $\text{R} = \text{hydrocarbon } \text{C}_x\text{H}_y$, and $x, y \in \mathbb{N}$.

dominate the CHOMg chemical compositions (>80%, Fig. 2C and Fig. S34) with a prevalence of nearly saturated aliphatics R, including long alkyl chains, which is uncommon for meteoritic soluble organic matter (6). The sequential traces of the CHOMg compositional space of the other three meteorites, Novato, Chelyabinsk, and Murchison, demonstrate their wide molecular ranges and diversity (Fig. S3).

Dihydroxymagnesium Carboxylates: A Previously Unreported Chemical Class. To establish the chemical structure responsible for those peaks, the most intense mass peaks of MgO_4R^- compounds ($\text{R} = \text{hydrocarbon } \text{C}_x\text{H}_y$ and $x, y \in \mathbb{N}$) were subjected to collision-induced dissociation tandem mass spectrometry (CID-MS/MS) to initiate fragmentation. These CHOMg compounds were found to be highly thermostable. High collision energies (>10 eV, 965 kJ/mol) were necessary to observe $\text{Mg}(\text{OH})_2$ abstraction [$\Delta m/z = 57.99052$ atomic mass units (amu), Fig. S4] from the parent ions. Fragmentation patterns were characteristic of long-chain aliphatic compounds [$\Delta m/z = 2.01565$ amu for H_2 loss and $\Delta m/z = 28.03130$ amu for C_2H_4 elimination (27), Fig. S4]. Acidification of the samples caused Mg-metalorganics (organomagnesium complexes) to hydrolyze. The precipitation of $\text{Mg}(\text{OH})_2$ substantiates the idea that the observed CHOMg molecules are $[(\text{OH})_2\text{MgO}_2\text{CR}]^-$ anionic complexes (Fig. S4), namely dihydroxymagnesium carboxylates, which have not been reported to date in chemical databases (e.g., ChemSpider, SciFinder, and PubChem).

Thermodynamic properties of dihydroxymagnesium carboxylates were elucidated both experimentally and theoretically. Mass spectrometric and computed fragmentation energies are in agreement, indicating a remarkable stability of $[(\text{OH})_2\text{MgO}_2\text{CR}]^-$ as well as a strong (covalent) binding between $\text{Mg}(\text{OH})_2$ and the carboxyl group (Eqs. S1 and S3 and Table S2). The $[(\text{OH})_2\text{MgO}_2\text{CC}_{15}\text{H}_{31}]^-$ anion approaches a tetrahedral coordination geometry with Mg as coordination center (Fig. 3C). Interestingly, Mg atoms seem to occur in a rarely observed fourfold coordination (28). The reactivity of dihydroxymagnesium carboxylates as a function of chain length was assessed by determining Gibbs free energies ΔG for the reaction, shown in Eq. 1; ΔG was computed both by means of density functional theory (B3LYP-DFT) and by second-order Møller–Plesset perturbation theory (MP2):



The measured equilibrium constant K' [$K' \sim K \cdot c(\text{Mg}(\text{OH})_2)$, Eqs. S2 and S3] of the complex formation, following Eq. 1, relates to Gibbs free energy ΔG via Eq. 2:

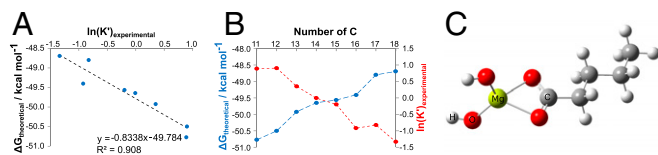


Fig. 3. Characterization of dihydroxymagnesium carboxylates. (A) The negative correlation between the experimental equilibrium constant, expressed as $\ln(K')$, and the computed Gibbs free energy ΔG of the $[(\text{OH})_2\text{MgO}_2\text{CC}_n\text{H}_{2n+1}]^-$ complex formation with $n \in \mathbb{N}$ for different linear alkyl chain lengths between C_{11} and C_{18} , as computed with density functional theory (DFT). (B) The dependency of $\ln(K')$ (experimentally via MS) and ΔG (theoretically via DFT) on different alkyl chain lengths is displayed to illustrate the reactivity of dihydroxymagnesium carboxylates, whereas the optimized computed geometry for the representative ion dihydroxymagnesium-*n*-pentanoate $[(\text{OH})_2\text{MgO}_2\text{CC}_4\text{H}_9]^-$ is depicted in C (see Table S2 for the computed coordinates of relaxed geometry of C_5 -dihydroxymagnesium carboxylate complex anion).

$$\Delta G = -RT \ln K'. \quad [2]$$

Eq. 2 provides a negative correlation of ΔG with K' (Fig. 3A and Fig. S5). The tendency of carboxylate complex formation continually decreases with increasing alkyl chain lengths R, as a result of two opposite effects. The inductive, bond-polarizing +I effect increases with higher numbers of alkyl carbons, making the carboxyl groups better nucleophiles, thereby shifting the equilibrium toward complex formation. However, the inverse effect of chain length on the acidity or the deprotonation potential of the ligand dominates. Here, longer alkyl chain carboxylates have higher potential to remain in their protonated form (RCOOH), which makes them weaker nucleophiles. Consequently, a higher coordination tendency for short-chain organic acids results (Fig. 3B), which was verified for various homologous series (Fig. S5).

Mass difference network analysis visualizes holistic chemical diversity of CHOMg in detail. In this data-driven analytical approach, nodes represent experimental m/z values (here, FT-ICR-MS data of NWA 7325 soluble organic matter) and edges (connections within the network) represent exact mass differences, which are equivalent to a net molecular formula of a chemical reaction (29). The chemical complexity/reactivity of the CHOMg space (pink-coded nodes) and its regular connection to certain CHO compositions (blue-coded nodes, Fig. 4A and Fig. S6) is revealed. Here, $\text{C}_x\text{H}_y\text{O}_z + \text{Mg}(\text{OH})_2$ reaction pairs (with $x, y, z \in \mathbb{N}$) were identified for various degrees of unsaturation and numbers of oxygen atoms. First, highly connected methylene-based homologous series can be observed (CH_2 as an edge) for the CHO and CHOMg compositional spaces, respectively. Second, different subseries with varying oxygen numbers are present. This functional network is split into five disconnected subnetworks, differing in their saturation states and laid out in the CH_2 vs. O directions. The degree of unsaturation (described via double-bond equivalent values, DBE) affects the reactivity of CHO compounds ($\text{C}_x\text{H}_y\text{O}_z + \text{Mg}(\text{OH})_2 \rightarrow \text{C}_x\text{H}_{y+2}\text{O}_{z+2}\text{Mg}$ reaction, with $x, y, z \in \mathbb{N}$); the number of possible reactions increases with increasing DBE. Saturated $\text{C}_x\text{H}_y\text{O}_2$ compounds (DBE = 1) almost exclusively react to MgO_4R^- compositions (like dihydroxymagnesium carboxylates, $\text{R} = \text{hydrocarbon } \text{C}_x\text{H}_y$ and $x, y \in \mathbb{N}$). With increasing numbers of DBE, additional varieties of organomagnesium complex formation become available due to increased numbers of isomers of CHO compounds. On average, the transition from Fig. 4A to Fig. 4B doubles the number of organomagnesium compounds (pink chains), representing an increase in chemical CHOMg complexity.

The presence of carbonyl and hydroxyl groups in meteoritic soluble organic matter has previously been demonstrated (1, 6). We propose the additional presence of β -hydroxy carbonyl functionalities for unsaturated compounds that are isomeric and vinylogous to carboxylic compositions. Unsaturated β -hydroxy ketones are stabilized via conjugation effects, which enhance the likelihood for alternating σ and π bonds within the aliphatic chain (Fig. 4F). The enol form is preferred, relative to the keto form, due to the presence of a pseudo ring, driven by hydrogen bonding. Additionally, keto–enol tautomerism explains the acidic character of β -hydroxy ketones. They are able to form chelate complexes (30), similar to organomagnesium coordination compounds. This alternative Mg coordination motif, compared with carboxylate ligands, may explain why highly unsaturated oxygenated CHO molecules react to CHOMg compositions. Further, the presence of two organic ligands enhances the probability of forming organomagnesium complexes, compared with one single organic educt class.

Chemosynthesis of CHOMg Compounds and the Link to Thermal History. One might ask about the origin of these organomagnesium compounds and whether the genesis of this compound class is coupled to the individual “history” of the various meteorites,

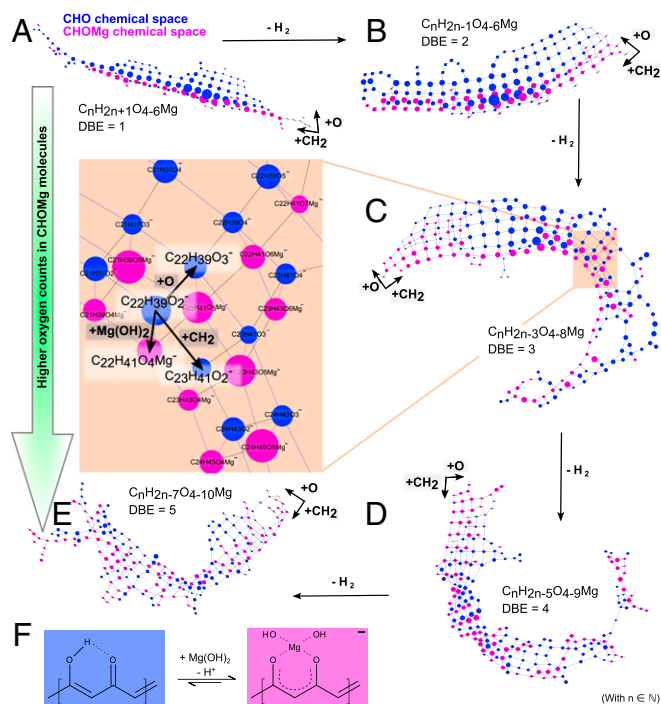


Fig. 4. Mass difference networks, presenting the chemical complexity/re-activity of the CHOMg space and its connection to CHO compositions. (A–E) Five subnetworks, each representing one distinct degree of unsaturation, as well as a gradual increase in the number of oxygen in CHOMg molecules, are shown for NWA 7325 soluble organic matter. The variance in unsaturation is expressed via DBE values. CHOMg nodes are pink and CHO nodes are blue. The nodal diameter is proportional to the natural logarithm of each mass peak's intensity. Three types of edges are defined, the mass differences of CH₂ and O illustrate the systematic connection within the CHO or CHOMg chemical space, and $\Delta m/z(\text{Mg}(\text{OH})_2)$ addresses reaction pairs that connect CHO and CHOMg compositions. (F) Proposed alternative organomagnesium complex formation with unsaturated β -hydroxy ketones as chelate ligands.

meteoroids, and parent bodies. The effects of shock events, thermal metamorphism, and aqueous alteration play a major role in the classification of meteorites, which are commonly based on petrologic indicators (31). CM-type meteorites (5, 32) have shown the highest number of CHNOS compositions. The thermally altered Sutter's Mill shows losses of these signatures with additional new polysulfidic patterns (33). The recent falls of the ordinary chondrites, such as Novato (L6), Chelyabinsk (LL5), or Vicência (LL3.2), show similar losses in nitrogen and sulfur compounds. Conversely, formation of compounds with high numbers of nitrogen at higher shock levels (23, 24, 34) are observed, suggesting that shock events/thermal metamorphism play a role in this context as well.

The CHOMg signatures relate to shock stage (with S0 being unshocked and S5 highly shocked meteorites, as assigned for examples in Fig. 5) and thermal processing among 61 meteorites of various classes, as demonstrated by orthogonal partial least square regression analysis (OPLS) (Fig. 5, *x* axis as first component). For example, the thermally altered meteorite Soltmany (35) contains >700 CHOMg compounds. In comparison, the less-altered meteorite Paris (CM) with only weak thermal alteration (36) shows merely 90 CHOMg compounds of low mass peak intensity. The information on the variation of oxygen numbers within CHOMg formulas is revealed by the *y* axis (orthogonal to the first component) of the OPLS analysis. Based on the mass difference network analysis (Fig. 4), we propose that the *y* axis potentially also represents a discrimination of the degree of unsaturation. High oxygen numbers of CHOMg molecular formulas correspond to a higher degree of unsaturation.

Parent body thermal metamorphism also imposes a compositional variance of CHOMg compounds. High thermal metamorphism is associated with an elevated saturation (high H/C ratio) and a convergence of oxygen numbers to 4 within the organomagnesium molecules at high thermal stress (Fig. S6). By heating Murchison, a meteorite with a low degree of metamorphism, we were able to simulate and follow the effect of short-duration thermal stress in a laboratory experiment. Here, CHOMg-based hierarchical cluster analysis revealed differentiation according to temperature regimes (Fig. S7). Similarly, the number of oxygen atoms in CHOMg molecules converges toward O = 4 at high temperatures, as expected (Fig. S7). A detailed comparison within highly shocked/thermally stressed ureilite meteorites also agrees with the above results (Fig. S7).

The production of CHOMg compounds by heating is further demonstrated by analyses of meteorite's fusion crust. Freshly fallen meteorites are found with a glassy coating that formed at ~1,400 °C surrounding their cold interior. The fusion crust is formed upon atmospheric entry by melting the meteoroid's surface as it enters the Earth's atmosphere at supersonic speed. During the brief melting, the liquid-like crust loses volatile elements and reacts with atmospheric matter faster, relative to the heterogeneous solid-state interior. ESI-FT-ICR mass spectra were acquired for Maribo (CM2) and Allende (CV3) by probing their outer crust and their inner core. Higher numbers and higher molecular diversity of CHOMg compounds were obtained from the crusted surfaces, relative to the core regions (Fig. S8). The different thermal conditions experienced by the outer and inner parts of a meteorite lead to different potential chemical activities, which promote the synthesis of these organomagnesium compounds at elevated temperatures within a short time scale. This observation agrees with the above experimental results, demonstrating that reaction energy, namely pressure and temperature, as substantiated by Eq. 2, relate with higher abundance of CHOMg molecules.

The role of alteration can also be evaluated from the isotopic signature of the Mg atoms in CHOMg compounds. Isotopic analyses of Mg were performed on both organic extracts and residual fractions of NWA 7325 and Novato (Fig. S1). The organic extract of Novato had a $\delta^{26}\text{Mg}$ value of $-0.74 \pm 0.08 \text{ ‰}$, and the residue had a $\delta^{26}\text{Mg}$ value of $-0.29 \pm 0.09 \text{ ‰}$. Details on the Mg isotopic analysis are given in *SI Materials and Methods*. Similarly, the organic extract of NWA 7325 had a $\delta^{26}\text{Mg}$ value of $-0.62 \pm 0.04 \text{ ‰}$, and the residue had a $\delta^{26}\text{Mg}$ value of $-0.35 \pm 0.11 \text{ ‰}$. Thus, for both Novato and NWA 7325, the organic extracts were relatively enriched in isotopically light Mg, compared with the isotopic composition of Mg in the bulk rock. This is consistent with the observation by Black et al. (37), who found chelation during intracellular processes enrich light Mg isotopes.

However, Mg isotopic fractionation occurs upon abiotic aqueous alteration as well. Aqueous alteration leads to clay-mineral formation and Mg-rich phases (11). We did not observe any significant direct correlation between the numbers of organomagnesium compounds and the extent of aqueous alteration within CM2 meteorites, ranging from CM2.7 to CM2.0 (Fig. S8). Studies from Wimpenny et al. (38) show that the removal of exchangeable magnesium from alteration phases preferentially liberates isotopically light Mg, compared with the bulk mineral. This suggests that aqueous alteration may have an indirect effect on the synthesis of organomagnesium compounds. If a released Mg educt, produced by aqueous alteration, is consecutively exposed to high temperatures, enhanced CHOMg formation would be expected to result by close spatial proximity and intercalation of the mineral and organic phases in CM2 meteoritic materials (11). Secondary ion mass spectrometric (SIMS) analyses of the Chelyabinsk meteorite indicated a spatial proximity of Mg and organic compounds (Fig. S1), which has not been reported previously by this method. Ordinary chondrites do not typically undergo aqueous alteration.

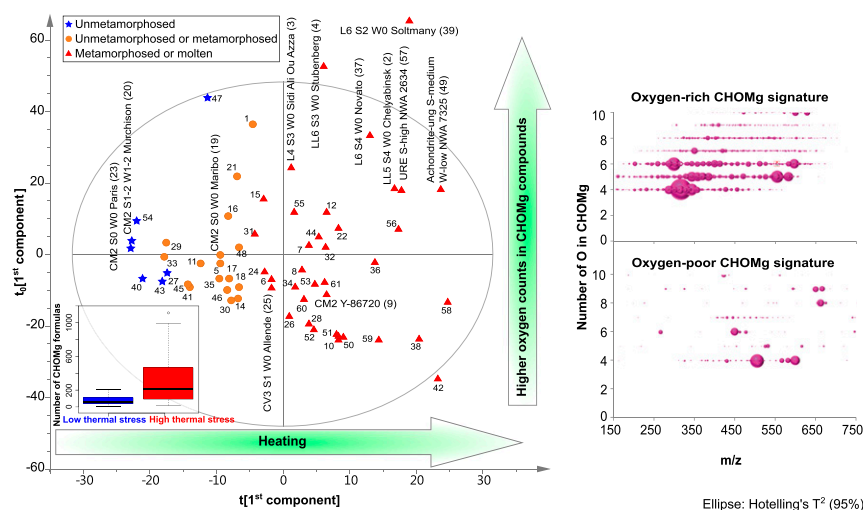


Fig. 5. Relationship of CHOMg signatures with different thermal processing stages of meteorites. An OPLS score scatter plot for 61 meteorites (CI, CK, CM, CO, CR, CV, EUC, H, L, LL, URE, and achondrite classes) with different inter- and intrameteorite class metamorphism stages is shown, based on the abundance and molecular diversity of CHOMg compounds. Details on the OPLS analysis are given in *SI Materials and Methods* and meteorite assignments are listed in *Table S1*. The box plots represent the averaged numbers of CHOMg molecular formulas for low and highly thermally altered meteorites, respectively. Thermal processing states vary from low to high along the x axis (first component), proceeding from negative to positive values. This first component (x axis) is related to the number and intensity of CHOMg molecular formulas, as represented in the box plot. The y axis (orthogonal to the first component) represents the proportion of oxygen atoms within the molecular formulas, as illustrated by modified van Krevelen diagrams of the most relevant loading values. Independent of the specimen, CHOMg signatures were observed with increased Mg-metalorganic diversity for thermally stressed meteorites. The two CM2 chondrites, Y-793321 and Y-86720, reported to be thermally metamorphosed (39), well-described meteorites, with respect to their shock history [Chelyabinsk (24) and Novato (23)], as well as the recently classified fall Sidi Ali Ou Azza (L4) and a very new German fall Stubenberg (LL6) were also assigned to the thermally stressed region.

The composition of soluble CHOMg compounds is shown to be highly related to the thermal-processing states of meteorites. Molecular complexity of MgO_4R^- compositions ($\text{R} = \text{hydrocarbon } \text{C}_x\text{H}_y$ and $x, y \in \mathbb{N}$) is increasingly diversified, because a meteorite experiences increasing degrees of thermal processing. The most abundant subclass of CHOMg compounds in meteorites is the four-oxygen-containing MgO_4R^- type and represents the previously unreported chemical class of dihydroxymagnesium carboxylates $[(\text{OH})_2\text{MgO}_2\text{CR}]^-$.

The use of CHOMg compound distributions as potential chemical markers, together with the CHNOS chemical space, may help to expand our knowledge of (i) astrochemistry of higher molecular masses and chemical complexity within the solar nebula and/or (ii) postaccretionary processes in meteoritic parent body metamorphism. In the context of meteorite classification, CHOMg content and diversity may provide a useful estimate of the degree of thermal alteration reflecting their temporal evolution under high temperature.

Additionally, this work raises the questions of whether these CHOMg compositions are specific for extraterrestrial chemistry and what we can learn from these findings within ongoing studies on natural metalorganic compounds in terrestrial systems and deep carbon sequestration in the Earth interior under high temperature and pressures (17).

Metal ions are essential for the origin of living systems on Earth (40–42). Metal ions can either support reactions via catalytic effects or stabilize organic molecules, because life-relevant organics are often thermolabile and celestial bodies undergo high-energy gradients through time and space. Here, highly thermostable organomagnesium compounds might have contributed to the stabilization of organic molecules, such as fatty acids, on a geological time scale, being in contact with Mg-bearing minerals at high energetic conditions. These protecting metalorganic motifs might represent important intermediate molecules in the selection history of organic molecules of life. A concentration/fractionation of fatty acids can be accomplished via the stabilization in their organomagnesium motifs, which is highly relevant in the formation of protocells/cells due to compartmentization/vesicle formation in membranes.

Due to their high abundance (13) and known metalorganic chemistry, Fe, Ni, Al, Zn, and V (9, 43, 44) may also be present as astrobiologically relevant molecular building blocks in meteorites, next to Mg-bearing compounds. No other metalorganics could be experimentally detected yet.

Potential future detections of organometallic compounds (or organics in general) from sample return missions to Mars, asteroids, or the Moon would imply that meteoritic organic compounds might survive some of the high-temperature, early phases of planetary accretion processes. This may not necessarily mean that life existed at a certain point in the histories of these planetary bodies. Insights into potential amplification of abiogenesis probabilities among planetary systems with various chemistries and molecular complexities can be achieved.

Materials and Methods

For ESI-FT-ICR-MS experiments, fragments of fresh interior samples were first washed by stirring for a few seconds within the extraction solvent (methanol, LC-MS grade; Fluka) before crushing in 1 mL solvent poured into the corresponding agate mortar. This procedure was shown to limit the number of peaks resulting from terrestrial and human contamination, for example fatty acids arising from sample handling. The mixture (suspension) was transferred into an Eppendorf vial and underwent ultrasonic cleaning for ≤ 10 min and then was centrifuged. The supernatant liquid was removed with a microsyringe, ready for flow injection into the ESI source. A solvent methanolic blank was measured in accordance to be able to detect indigenous meteoritic (metal)organic matter in each sample. Organomagnesium compounds were absent in blank spectra. Further details are given in *SI Materials and Methods*.

ACKNOWLEDGMENTS. We thank Rainer Bartoschewitz, Maria Elizabeth Zucolotto, Ansgar Greshake, Herbert Raab, Michael Farmer, Greg Hupé, André Moutinho, Sonny Clary, Fabien Kuntz, Valery Bogdanovsky, Aid Mohamed, Ismailly Sidi Mohamed, Abdel Fattah Gharrad, and the National Institute of Polar Research for providing meteorite samples. We also thank the reviewers for their open-mindedness regarding our concept and their constructive comments, which substantially improved the quality of the manuscript, and Matthew Sanborn for proofreading the manuscript. This work was supported by NASA Cosmochemistry Grant NNX14AM62G and Emerging Worlds Grant NNX16AD34D (to Q.-Z.Y.).

1. Sephton MA (2002) Organic compounds in carbonaceous meteorites. *Nat Prod Rep* 19(3):292–311.
2. Cronin JR, Pizzarello S (1997) Enantiomeric excesses in meteoritic amino acids. *Science* 275(5302):951–955.
3. Cooper G, et al. (2001) Carbonaceous meteorites as a source of sugar-related organic compounds for the early Earth. *Nature* 414(6866):879–883.
4. Meierhenrich UJ, Muñoz Caro GM, Bredehöft JH, Jessberger EK, Thiemann WH-P (2004) Identification of diamino acids in the Murchison meteorite. *Proc Natl Acad Sci USA* 101(25):9182–9186.
5. Schmitt-Kopplin P, et al. (2010) High molecular diversity of extraterrestrial organic matter in Murchison meteorite revealed 40 years after its fall. *Proc Natl Acad Sci USA* 107(7):2763–2768.
6. Hertkorn N, Harir M, Schmitt-Kopplin P (2015) Nontarget analysis of Murchison soluble organic matter by high-field NMR spectroscopy and FTICR mass spectrometry. *Magn Reson Chem* 53(9):754–768.
7. Cody GD, Alexander CO, Tera F (2002) Solid-state (^1H and ^{13}C) nuclear magnetic resonance spectroscopy of insoluble organic residue in the Murchison meteorite: A self-consistent quantitative analysis. *Geochim Cosmochim Acta* 66(10):1851–1865.
8. Burton AS, Stern JC, Elsila JE, Glavin DP, Dworkin JP (2012) Understanding prebiotic chemistry through the analysis of extraterrestrial amino acids and nucleobases in meteorites. *Chem Soc Rev* 41(16):5459–5472.
9. Fioroni M (2016) Astro-organometallics of Fe, Co, Ni: Stability, IR fingerprints and possible locations. *Comput Ther Chem* 1084:196–212.
10. Ehrenfreund P, Glavin DP, Botta O, Cooper G, Bada JL (2001) Extraterrestrial amino acids in Orgueil and Ivuna: Tracing the parent body of CI type carbonaceous chondrites. *Proc Natl Acad Sci USA* 98(5):2138–2141.
11. Le Guillou C, Bernard S, Brearley AJ, Remusat L (2014) Evolution of organic matter in Orgueil, Murchison and Renazzo during parent body aqueous alteration: In situ investigations. *Geochim Cosmochim Acta* 131:368–392.
12. Yesiltas M, Kebukawa Y (2016) Associations of organic matter with minerals in Tagish Lake meteorite via high spatial resolution synchrotron-based FTIR microspectroscopy. *Meteorit Planet Sci* 51(3):584–595.
13. Lodders K (2003) Solar system abundances and condensation temperatures of the elements. *Astrophys J* 591(2):1220–1247.
14. Elschenbroich C, Salzer A (1989) *Organometallics* (Wiley-VCH, New York).
15. Khairallah GN, Thum CC, Lesage D, Tabet J-C, O'Hair RA (2013) Gas-phase formation and fragmentation reactions of the organomagnesates $[\text{RMgX}_2]^-$. *Organometallics* 32(8):2319–2328.
16. Bock CW, Kaufman A, Glusker JP (1994) Coordination of water to magnesium cations. *Inorg Chem* 33(3):419–427.
17. Hazen RM, Jones AP, Baross JA (2013) Carbon in earth. Available at minsocam.org/MSA/Rim/RiMG075/RiMG075_Title_Page.pdf. Accessed December 27, 2016.
18. Schulte M, Shock E (2004) Coupled organic synthesis and mineral alteration on meteorite parent bodies. *Meteorit Planet Sci* 39(9):1577–1590.
19. Ferralis N, Matys ED, Knoll AH, Hallmann C, Summons RE (2016) Rapid, direct and non-destructive assessment of fossil organic matter via microRaman spectroscopy. *Carbon* 108:440–449.
20. Johnson NM, Elsila JE, Kopstein M, Nuth JA (2012) Carbon isotopic fractionation in Fischer-Tropsch-type reactions and relevance to meteorite organics. *Meteorit Planet Sci* 47(6):1029–1034.
21. Hill HG, Grady CA, Nuth JA, 3rd, Hallenbeck SL, Sitko ML (2001) Constraints on nebular dynamics and chemistry based on observations of annealed magnesium silicate grains in comets and in disks surrounding Herbig Ae/Be stars. *Proc Natl Acad Sci USA* 98(5):2182–2187.
22. Irving AJ, et al. (2013) Ungrouped mafic achondrite Northwest Africa 7325: A reduced, iron-poor cumulate olivine gabbro from a differentiated planetary parent body. Available at www.lpi.usra.edu/meetings/lpsc2013/pdf/2164.pdf.
23. Jenniskens P, et al. (2014) Fall, recovery, and characterization of the Novato L6 chondrite breccia. *Meteorit Planet Sci* 49(8):1388–1425.
24. Popova OP, et al.; Chelyabinsk Airburst Consortium (2013) Chelyabinsk airburst, damage assessment, meteorite recovery, and characterization. *Science* 342(6162):1069–1073.
25. Summons RE, Albrecht P, McDonald G, Moldowan JM (2008) Molecular biosignatures. *Space Sci Rev* 135(1–4):133–159.
26. Wakil SJ (1989) Fatty acid synthase, a proficient multifunctional enzyme. *Biochemistry* 28(11):4523–4530.
27. Cheng C, Gross ML (2000) Applications and mechanisms of charge-remote fragmentation. *Mass Spectrom Rev* 19(6):398–420.
28. Dove AP, et al. (2003) Low coordinate magnesium chemistry supported by a bulky β -diketiminato ligand. *Dalton Trans* (15):3088–3097.
29. Tziotis D, Hertkorn N, Schmitt-Kopplin P (2011) Kendrick-analogous network visualisation of ion cyclotron resonance Fourier transform mass spectra: Improved options for the assignment of elemental compositions and the classification of organic molecular complexity. *Eur J Mass Spectrom (Chichester)* 17(4):415–421.
30. Stary J, Liljenzin JO (1982) Critical evaluation of equilibrium constants involving acetylacetone and its metal chelates. *Pure Appl Chem* 54(12):2557–2592.
31. Huss GR, Rubin AE, Grossman JN (2006) Thermal metamorphism in chondrites. *Meteor Early Sol Syst* 11:567–586.
32. Haack H, et al. (2012) Maribo-A new CM fall from Denmark. *Meteorit Planet Sci* 47(1):30–50.
33. Jenniskens P, et al.; Sutter's Mill Meteorite Consortium (2012) Radar-enabled recovery of the Sutter's Mill meteorite, a carbonaceous chondrite regolith breccia. *Science* 338(6114):1583–1587.
34. Keil K, et al. (2015) The Vicência meteorite fall: A new unshocked (S1) weakly metamorphosed (3.2) LL chondrite. *Meteorit Planet Sci* 50(6):1089–1111.
35. Schmitt-Kopplin P, et al. (2012) Chemical footprint of the solvent soluble extraterrestrial organic matter occluded in Soltmany ordinary chondrite. *Meteorites* 2(1–2):71–92.
36. Martins Z, Modica P, Zanda B, d'Hendecourt LLS (2015) The amino acid and hydrocarbon contents of the Paris meteorite: Insights into the most primitive CM chondrite. *Meteorit Planet Sci* 50(5):926–943.
37. Black JR, Yin Q, Casey WH (2006) An experimental study of magnesium-isotope fractionation in chlorophyll-a photosynthesis. *Geochim Cosmochim Acta* 70(16):4072–4079.
38. Wimpenny J, Colla CA, Yin Q-Z, Rustad JR, Casey WH (2014) Investigating the behaviour of Mg isotopes during the formation of clay minerals. *Geochim Cosmochim Acta* 128:178–194.
39. Tonui E, et al. (2014) Petrographic, chemical and spectroscopic evidence for thermal metamorphism in carbonaceous chondrites I: CI and CM chondrites. *Geochim Cosmochim Acta* 126:284–306.
40. Williams RJ (2007) Systems biology of evolution: The involvement of metal ions. *Biometals* 20(2):107–112.
41. Martin W, Russell MJ (2003) On the origins of cells: A hypothesis for the evolutionary transitions from abiotic geochemistry to chemoautotrophic prokaryotes, and from prokaryotes to nucleated cells. *Philos Trans R Soc Lond B Biol Sci* 358(1429):59–83, discussion 83–85.
42. Saladino R, Botta G, Bizzarri BM, Di Mauro E, Garcia Ruiz JM (2016) A global scale scenario for prebiotic chemistry: Silica-based self-assembled mineral structures and formamide. *Biochemistry* 55(19):2806–2811.
43. Witt M, Roesky HW (2000) Organoaluminum chemistry at the forefront of research and development. *Curr Sci* 78:410–430.
44. Rehder D (2008) Is vanadium a more versatile target in the activity of primordial life forms than hitherto anticipated? *Org Biomol Chem* 6(6):957–964.
45. Senior JK (1951) Partitions and their representative graphs. *Am J Math* 73(3):663–689.
46. Frisch MJ, et al. (2004) Gaussian 03, revision c. 02 (Gaussian, Inc., Pittsburgh).
47. Foresman JB, Frisch AE (1993) *Exploring Chemistry with Electronic Structure Methods: A Guide to Using Gaussian* (Gaussian, Inc., Pittsburgh).
48. Jensen F (2002) Polarization consistent basis sets. III. The importance of diffuse functions. *J Chem Phys* 117(20):9234–9240.
49. Schlegel HB (1982) Optimization of equilibrium geometries and transition structures. *J Comput Chem* 3(2):214–218.
50. Schlegel HB (1984) Estimating the Hessian for gradient-type geometry optimizations. *Theor Chim Acta* 66(5):333–340.
51. Császár P, Pulay P (1984) Geometry optimization by direct inversion in the iterative subspace. *J Mol Struct* 114:31–34.
52. Kanawati B, Joniec S, Winterhalter R, Moortgat GK (2007) Mass spectrometric characterization of small oxocarboxylic acids and gas phase ion fragmentation mechanisms studied by electrospray triple quadrupole-MS/MS-TOF system and DFT theory. *Int J Mass Spectrom* 266(1):97–113.
53. Gabelica V, Galic N, Rosu F, Houssier C, De Pauw E (2003) Influence of response factors on determining equilibrium association constants of non-covalent complexes by electrospray ionization mass spectrometry. *J Mass Spectrom* 38(5):491–501.
54. Davis AM (2005) *Meteorites, Comets, and Planets: Treatise on Geochemistry* (Elsevier, Amsterdam), 2nd Ed.
55. Shannon P, et al. (2003) Cytoscape: A software environment for integrated models of biomolecular interaction networks. *Genome Res* 13(11):2498–2504.
56. Lucio M, Fekete A, Frommberger M, Schmitt-Kopplin P (2011) Metabolomics: High-resolution tools offer to follow bacterial growth on a molecular level. *Handbook of Molecular Microbial Ecology Metagenomics I: Metagenomics and Complementary Approaches*, ed de Bruijn FJ (Wiley, New York), pp 683–695.
57. Jacobsen B, et al. (2008) ^{26}Al - ^{26}Mg and ^{207}Pb - ^{206}Pb systematics of Allende CAIs: Canonical solar initial $^{26}\text{Al}/^{27}\text{Al}$ ratio reinstated. *Earth Planet Sci Lett* 272(1–2):353–364.
58. Young ED, Galy A (2004) The isotope geochemistry and cosmochemistry of magnesium. *Rev Mineral Geochem* 55(1):197–230.
59. Galy A, et al. (2003) Magnesium isotope heterogeneity of the isotopic standard SRM980 and new reference materials for magnesium-isotope-ratio measurements. *J Anal At Spectrom* 18(11):1352–1356.
60. Li W-Y, et al. (2010) Heterogeneous magnesium isotopic composition of the upper continental crust. *Geochim Cosmochim Acta* 74(23):6867–6884.
61. Bourdon B, Tipper ET, Fitoussi C, Stracke A (2010) Chondritic Mg isotope composition of the Earth. *Geochim Cosmochim Acta* 74(17):5069–5083.
62. Rubin AE (2006) Shock, post-shock annealing, and post-annealing shock in ureilites. *Meteorit Planet Sci* 41(1):125–133.